DOI: 10.1002/ejic.200700534

Crystal Structure, Electrochemical and Optical Properties of $[Au_9(PPh_3)_8](NO_3)_3$

Fei Wen,[a] Ulli Englert,[a] Benjamin Gutrath,[a] and Ulrich Simon*[a]

Keywords: Gold clusters / Nanoparticles / Optical properties / Electrochemistry / Band gap

The single-crystal structure of $[Au_9(PPh_3)_8](NO_3)_3$ was resolved for the first time with atomic resolution. The cluster has crystallographic D_2 and approximate molecular D_{2h} skeletal symmetry derived from an icosahedron. Voltammetry of the Au_9 clusters in CH_2Cl_2 reveals a 1.78-eV energy gap between the first one-electron oxidation peak and the first reduction peak. The UV/Vis and luminescence properties of Au_9 clusters were also investigated. The cluster solid shows two broad emission peaks at 579 nm and 853 nm, respectively, at room temperature.

Introduction

Research on gold nanoparticles with a size of a few nanometres has been of great interest in recent years. Owing to the spatial confinement of the charge carriers in these small particles, the valance and conduction bands split into discrete, quantized electronic levels.[1] Thus the electric properties of these small gold nanoparticles evolve from the state of bulk continuum to discrete molecular orbital energy levels, which makes them particularly attractive for application in nanodevices and molecular electronics.[2]

Much effort has been directed towards exploring the size range for gold nanoparticles in which the transition from bulk to molecular behaviour becomes evident. Transition from redox molecule-like charging to bulk metal-like double-layer capacitive charging was observed in voltammetric and near-IR studies of different-sized Au clusters coated with alkanethiolate monolayers.[1a] With an increase from 1.1 to 1.9 nm in diameters, the HOMO–LUMO (the highest occupied and lowest unoccupied molecular orbitals) energy gap decreases from 0.9 to 0.4 eV. Furthermore, numerous studies have reported photoluminescence in gold clusters with diameters below 5 nm;[3] this is believed to be a consequence of quantization of the electronic levels in the cluster cores and indicates the molecule-like behaviour of the clusters.

Various methods have been reported for the preparation of Au nanoparticles. One of the best-known methods of preparing Au clusters with subnanometre size is using sodium borohydride to reduce gold salts in the presence of triarylphosphanes. Synthesis and characterization of enneanuclear gold clusters $[Au_9(PAr_3)_8]Y_3$, where PAr_3 is a phosphane ligand and Y is a noncoordinating anion, have been well documented in the literature.[4] Only a few of them could be crystallized and examined with single-crystal X-ray diffraction, which enables a precise determination of the structure of the cluster core with ligand shell. However, the full X-ray structure of pure $[Au_9(PPh_3)_8](NO_3)_3$ is still unknown because of the poor crystal quality. This problem has most recently partially been overcome by forming a supramolecular intercluster compound consisting of the $Au_9(PPh_3)_8^{3+}$ cluster and $[PW_{12}O_{40}]^{3-}$ Keggin anions.[5]

In a previous communication we preliminarily presented the core structure of $[Au_9(PPh_3)_8]^{3+}$.[6] In this report we are able to present the single-crystal data, and electrochemical and optical properties of $[Au_9(PPh_3)_8](NO_3)_3$ as a methanol solvate in full detail. In particular, for the first time the band gap was determined from the differential pulse voltammetry (DPV) measurements. Furthermore, the molecule-like nature of the Au_9 clusters was proven by photoluminescence measurements at room temperature.

Results and Discussion

Single-Crystal Structure

Although the crystal structures of some Au_9 clusters have already been reported in the literature, their precise determinations were generally limited by disordering of the phosphane ligands bonded on Au atoms. Furthermore, the soft potential energy surface that interconnects the skeletal isomers of the cluster compound makes isolating good-sized single crystals very problematic.[7] Therefore, for most known Au_9 clusters only the metal core and phosphorus atoms have been defined. In this work, the preparation of **1** was performed by $NaBH_4$ reduction of $Au(PPh_3)NO_3$ according to a literature method.[8a] After reduction, the red-

[a] Institute for Inorganic Chemistry, RWTH Aachen University, Landoltweg 1, 52074 Aachen, Germany
Fax: +49-241-8099003
E-mail: ulrich.simon@ac.rwth-aachen.de

brown residue was copiously washed with tetrahydrofuran and hexane, yielding a green powder. TEM analyses revealed that larger Au particles, if formed during synthesis of **1**, were washed away in this step owing to their uncharged cores. As shown in Figure 1, the samples obtained only contained particles with a diameter of about 1 nm.

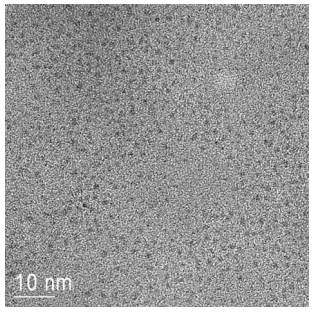

Figure 1. TEM image of cluster **1**.

Further recrystallization in methanol/ether led to the formation of dark green crystals, which were examined by X-ray analysis and are shown in Figure 2. The positional parameters are listed in Table 1, while the selected bond lengths and angles are summarized in Table 2. The cluster has crystallographic D_2 and approximate molecular D_{2h} skeletal symmetry, very similar to $[Au_9\{P(p\text{-}C_6H_4CH_3)_3\}_8](PF_6)_3$,[8b] which is derived from the centred icosahedron by removing a rectangle of four gold atoms. Each unit cell contains four Au_9 cluster cations, eight well-ordered nitrate anions and 16 methanol molecules. A third anion and an additional solvent molecule per cluster are disordered and occupy residual voids in the structure. Thus, the composition of the single crystal examined corresponds to the stoichiometry $\mathbf{1}\cdot 5CH_3OH$.

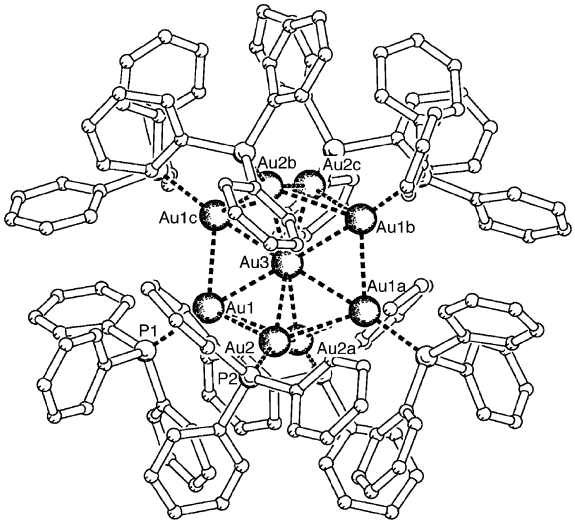

Figure 2. Structure of the $[Au_9(PPh_3)_8]^{3+}$ cluster cation (PLATON[10a]) in single-crystal $\mathbf{1}\cdot 5CH_3OH$. Symmetry codes, a: x, 0.5 – y, z; b: x, 0.5 – y, 0.5 – z; c: –x, y, 0.5 – z.

Table 1. Atomic coordinates ($\times 10^4$) and equivalent isotropic displacement parameters [$\times 10^3$ (Å)^2] for cluster $\mathbf{1}\cdot 5CH_3OH$.[a]

	x	y	z	U_{eq}
Au1	88(1)	1650(1)	1790(1)	23(1)
Au2	533(1)	2555(1)	1310(1)	24(1)
Au3	0	2500	2500	16(1)
P1	144(2)	965(2)	1110(4)	29(1)
P2	1318(2)	2554(2)	777(4)	28(1)
N1	2500	0	3460(3)	82(15)
O1	2500	0	2810(4)	150(2)
O2	2832(19)	218(18)	3710(3)	158(17)

[a] U_{eq} is defined as one-third of the trace of the orthogonalized U_{ij} tensor.

Table 2. Selected bond lengths [Å] and angles [°] for cluster $\mathbf{1}\cdot 5CH_3OH$.[a]

Au1–Au2	2.8804(12)	Au3–Au2c	2.6746(9)
Au1–Au3	2.7078(9)	Au3–Au2b	2.6746(9)
Au2–Au3	2.6746(9)	Au3–Au1c	2.7078(9)
Au1–Au1	2.7718(19)	Au3–Au1a	2.7078(8)
Au1–Au2a	2.8547(12)	Au3–Au1b	2.7079(8)
Au2–Au2a	2.7624(17)		
Au2–Au1a	2.8547(12)	Au1–P1	2.292(6)
Au3–Au2a	2.6745(9)	Au2–P2	2.271(6)
P1–Au1–Au3	175.45(18)	Au2a–Au2–Au1a	61.67(3)
P1–Au1–Au1c	124.96(18)	P2–Au2–Au1	119.92(16)
Au3–Au1–Au1c	59.22(2)	Au3–Au2–Au1	58.21(2)
P1–Au1–Au2a	118.40(18)	Au2a–Au2–Au1	60.74(3)
Au3–Au1–Au2a	57.40(2)	Au1a–Au2–Au1	109.19(4)
Au1c–Au1–Au2a	103.14(3)	Au2a–Au3–Au2	62.19(4)
P1–Au1–Au2	119.74(17)	Au2a–Au3–Au2c	118.22(4)
Au3–Au1–Au2	57.09(2)	Au2–Au3–Au2c	173.58(3)
Au1c–Au1–Au2	112.41(3)	Au2–Au3–Au2b	118.22(4)
Au2a–Au1–Au2	57.59(4)	Au2a–Au3–Au1c	109.96(3)
P2–Au2–Au3	147.63(18)	Au2–Au3–Au1c	121.57(3)
P2–Au2–Au2a	152.49(18)	Au2c–Au3–Au1c	64.71(3)
Au3–Au2–Au2a	58.91(2)	Au2b–Au3–Au1c	64.06(3)
P2–Au2–Au1a	130.31(16)	Au1c–Au3–Au1a	170.39(3)
Au3–Au2–Au1a	58.54(3)	Au1–Au3–Au1a	119.35(4)

[a] Symmetry codes, a: x, 0.5 – y, z; b: x, 0.5 – y, 0.5 – z; c: –x, y, 0.5 – z.

As shown in Table 2, the radial Au–Au bond lengths lie in the range 2.6746(9)–2.7079(8) Å, which are slightly smaller than the values, 2.689(2)–2.735(2) Å, reported for $[Au_9\{P(p\text{-}C_6H_4OCH_3)_3\}_8](NO_3)_3$.[8c] The peripheral Au–Au distances are 2.7624(17)–2.8804(12) Å, which are larger than the radial distances and fall in the same range as 2.751(4)–2.899(4) Å reported for $[Au_9\{P(p\text{-}C_6H_4OCH_3)_3\}_8](NO_3)_3$.[8c] Using $[PW_{12}O_{40}]^{3-}$ as the anion and DMF/acetone as the solvent, the single crystal of the $[Au_9(PPh_3)_8]^{3+}$ cluster with a skeleton symmetry close to D_{2h} was obtained very recently by Jansen and co-workers.[5] They reported Au–Au distances ranging radially from 2.661(1) to 2.738(1) Å and peripherally from 2.788(1) to 2.926(1) Å, where the peripheral Au–Au bond lengths are slightly larger than those obtained in the present study. The Au–P bond lengths in $\mathbf{1}\cdot 5CH_3OH$ are 2.292(6) and 2.271(6) Å, respectively, which are comparable to the peripheral Au–P distances 2.29(3)–2.33(3) Å previously published for the $[Au_8(PPh_3)_7](NO_3)_2$ cluster.[9]

UV/Vis Spectroscopy

The diffusion reflectance spectrum of the cluster **1** in the solid state was recorded with the green crystals recrystallized from methanol/ether and shown in Figure 3. The spectrum is in good agreement with those obtained from other Au_9 green crystals, $[Au_9\{P(p\text{-}C_6H_4Me)_3\}_8](BF_4)_3$ and $[Au_9(PPh_3)_8](BF_4)_3$,[8b] which both have a D_{2h} skeletal symmetry derived from the centred icosahedron. However, when the green crystals as-prepared were redissolved in CH_2Cl_2 and dried on a glass slide in nitrogen, microcrystals with two different colours, green and red-brown, were observed under the microscope. While the green microcrystals give the same electronic spectral characteristics as measured before, the red-brown microcrystals show a different spectral shape, as shown in Figure 3. The latter accords with the spectrum observed from $[Au_9\{P(p\text{-}C_6H_4OMe)_3\}_8](BF_4)_3$, which contains the centred crown of gold atoms with a cluster symmetry very close to D_{4d}.[8b] Mingos and his coworkers have reported the presence of two skeletal isomers in $[Au_9\{P(p\text{-}C_6H_4OMe)_3\}_8](NO_3)_3$ cluster compounds.[8c] Jansen et al. also obtained $[Au_9(PPh_3)_8](PW_{12}O_{40})_3$ with two skeletal geometries by using a different combination of solvents.[5] Unfortunately, here we did not obtain the gold-brown crystals with a quality good enough for X-ray crystallographic measurement.

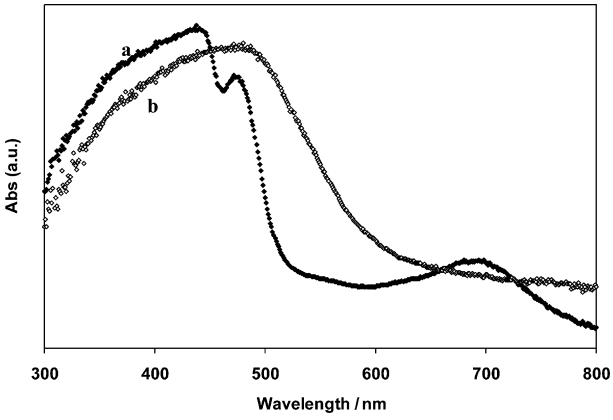

Figure 3. Diffuse reflectance spectra for cluster **1** in the solid state: (a) green crystals and (b) red-brown microcrystals.

For the Au clusters in solution state, the optical response in UV/Vis spectra has been widely used to probe their size-dependent electronic structures. With a size over 2 nm, the Au nanoparticles usually exhibit a surface plasmon band in the absorption spectra. When the particle sizes are less than 2 nm, the surface plasmon band becomes obscure, and finally only a smooth spectrum with absorbance increasing exponentially from the visible to the ultraviolet region can be observed.[1b,10] When the particle sizes further decrease to subnanometre range, the discrete peaks emerge in the UV/Vis spectra.[7]

Cluster **1** prepared in this work showed an identical optical spectrum in solution to the data published before.[7,11] As shown in Figure 4 (a), four discrete peaks were observed, indicating the presence of molecule-like electronic levels. The spectra are generally attributed to the intramolecular transitions of the $Au_9(PPh_3)_8^{3+}$ cluster framework. By assuming a D_{2h} skeletal symmetry of the $Au_9(PPh_3)_8^{3+}$ cluster in solution the same as that of the green crystals, Jaw and Mason[11a] interpreted the electronic absorption and magnetic circular dichroism (MCD) spectra in the UV/Vis range 607–278 nm with a simple molecular orbital (MO) scheme, which was primarily based on σ Au–Au interaction from 6s orbitals. Previous reports have suggested that these molecule-like transitions are extremely sensitive to the cluster core size and geometry, but not sensitive to the variation of phosphanes and anions.[7] Therefore these optical spectra are very helpful to analyze the core nuclearity of clusters in solution and to track the process of cluster degradation or aggregation reactions. In the present work, two ligand exchange reactions with cluster **1** were carried out to examine the stability of the Au core and explore the feasibility of replacing the bulky triphenyl phosphane ligands on the cluster surface.

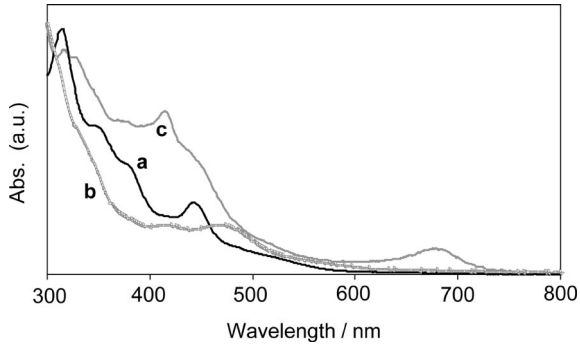

Figure 4. Electronic spectra of cluster **1** (a) in CH_2Cl_2; (b) after ligand exchange with TPPMS, in H_2O; (c) after ligand exchange with propanethiol, in CH_2Cl_2.

Parts b and c of Figure 4 illustrate the spectral differences of the cluster solution after ligand exchange with triphenylphosphane monosulfonate sodium salt (TPPMS) and propanethiol, respectively. The dissociative mechanism has been suggested previously when introducing new phosphane ligands to the $[Au_9(PPh_3)_8]^{3+}$ cluster solution.[9,12] Similarly, here a cluster solution with a UV spectrum consistent with that of Au_8 was obtained after a two-phase ligand exchange with TPPMS. The obtained water-soluble cluster solution showed one singlet resonance in $^{31}P\{^1H\}$ spectra at δ = 54.5 ppm in D_2O. As thiols usually have a more intensive interaction with gold than phosphanes,[13] a liable ligand exchange is expected to occur after introducing propanethiol to a cluster **1** solution. In the course of our studies, it is also observed that during the exchange process the original gold core changes. As shown in part c of Figure 4, the spectrum after ligand exchange exhibits characteristics similar to those reported for thiol-stabilized Au_{11} clusters.[14]

Photoluminescence

In addition to the UV/Vis absorbance studies, the luminescent spectra of cluster **1** in the solid state as well as in

CH_2Cl_2 were also recorded. The near-IR luminescence of small gold-containing clusters has been reported before,[3a,3b,15] which makes them promising for application in nanophotonics devices and as luminescent probes in medical imaging. The subnanometre clusters exhibit luminescence with higher quantum yields than the larger clusters because of their large energy-level gaps, which limits the contribution of nonradiative processes in relaxation. Figure 5 presents the photoluminescence spectrum of the solid at room temperature with an excitation at 532 nm. Two broad emission peaks were observed at 579 nm and 853 nm, respectively.

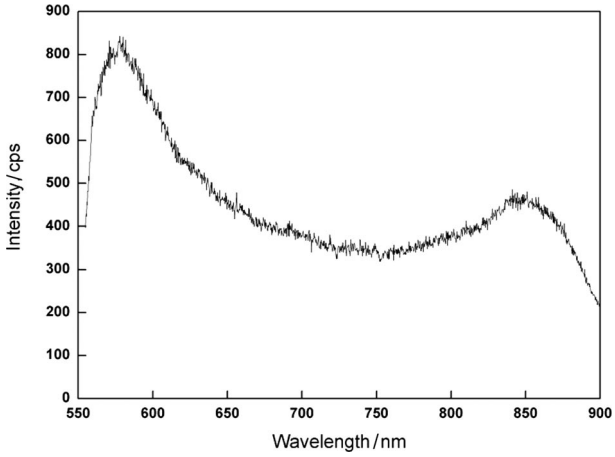

Figure 5. Emission spectrum of the cluster solid of **1** (excitation at 532 nm).

In previous work, Yam et al.[15e,15f] reported a dual luminescence centred at 500 nm and 700 nm for polynuclear Au^I-sulfido complexes with up to 12 Au atoms. Similarly, El-Sayed and Whetten also observed a very broad emission from a glutathione-stabilized Au_{28} cluster, which covers the visible to infrared range (620–1550 nm) with two maxima at around 800 and 1100 nm, respectively.[3b] In both works, the long wavelength emission was assigned to the phosphorescence originating from a triplet excited state of the Au clusters, while the short wavelength emission was attributed to the fluorescence from a singlet excited state. Recently, Bruce et al. observed an emission centred at 540 nm at 77 K with a metallamacrocyclic phosphane Au_9 thiolate cluster, whereas at room temperature this emission becomes very weak.[15a] In a very recent work Huang et al. reported the broad fluorescence of 2-nm Au clusters in solution with high quantum yield.[15g] While we observed the two broad emission peaks in the solid, in solution only a very weak emission signal at 630 nm could be recorded. The lack of the longer wavelength emission might be related to the structural isomerization the cluster undergoes in solution. A detailed analysis of this phenomenon will be part of our future work.

Electrochemistry

Cyclic (CV) and differential pulse (DPV) voltammetries have been widely used to investigate the properties of highly monodisperse semiconductor and metal nanoparticles, especially in order to evaluate the HOMO–LUMO energy gaps, which can be determined by the first oxidation and reduction peaks. As shown in Figure 6, a series of well-defined charging peaks are noticeably illustrated for cluster **1** in the potential range –2.0 to +2.0 V.

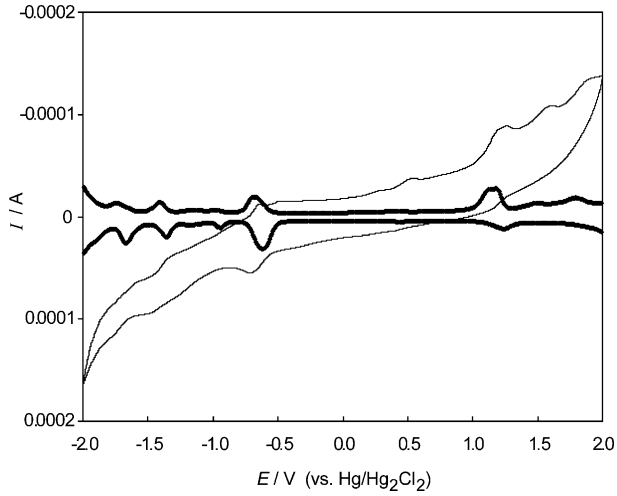

Figure 6. Cyclic and differential pulse voltammograms of 1.0 mM cluster **1** solution in CH_2Cl_2, with 0.1 M tetrabutylammonium hexafluorophosphate (TBHF) as a supporting electrolyte. The CV potential scan rate was 50 mV. The pulse amplitude was 50 mV.

The DPV voltammogram is in accordance with the CV data, but with a higher accuracy to resolve the redox current peaks because of the minimization of the charging-current effect. The distinct peaks shown in Figure 6 are ascribed to the discrete charging of the cluster molecules at the electrode surface. In an early report, van der Linden et al. performed a detailed electrochemical study of two-electron reduction of the $Au_9(PPh_3)_8(PF_6)_3$ cluster in various solvents.[16] By controlled potential electrolyses in acetonitrile at –0.60 V (vs. Ag–AgCl, 0.1 M LiCl-acetone), the unipositive $Au_9(PPh_3)_8PF_6$ cluster was obtained from the corresponding 3+ ion with a skeletal symmetry change from D_{2h} to D_3, where the potential is identical to the first reductive peak of cluster **1** observed in the present work, that is, –0.64 V (vs. Hg/Hg_2Cl_2, saturated KCl). Furthermore, according to the DPV curves in Figure 6, a substantial electrochemical gap of 1.78 eV can be easily derived from the first oxidation and reduction peaks, occurring at about 1.14 V and –0.64 V, respectively. This rather substantial spacing has been observed in numerous small-sized Au clusters and been accounted for by the emergence of a "molecule-like" HOMO–LUMO band gap in the nanoclusters with subnanometre dimensions.[1a,14b,17a,17b] Yang and Chen investigated the HOMO–LUMO gap of Au_{11} clusters stabilized with triphenylphosphane and found the value increased from 1.4 to 1.8 eV after ligand exchange with dodecanethiolate ligands.[14b] Quinn and co-workers reported a 1.2-eV gap from a hexanethiolate-coated Au_{38} cluster according to the voltammetric measurements.[17c] Previously, the electrochemical gaps for $Au_{13}[PPh_3]_4(SR)_2Cl_2$ and

$Au_{13}[PPh_3]_4(SR)_4$ were reported to be 1.6–1.7 eV,[17a] while for $Au_{11}Cl_3(PPh_3)_7$ it was 1.41 eV and after ligand exchange with *n*-dodecanethiols it increased to 1.76 eV.[14b] Herein, the voltammetry studies of cluster **1** show an almost identical electrochemical gap to that previously reported for the Au_{11} cluster.

Conclusion

The single-crystal structure of the $[Au_9(PPh_3)_8](NO_3)_3$ cluster was determined to be a green tetragonal modification that contains a cation that has D_{2h} skeletal symmetry derived from a centred icosahedron. The optical data and electrochemistry characterization revealed its molecule-like nature and a 1.78-eV HOMO–LUMO energy gap. Luminescence measurements of the cluster solid give two broad emissions with maxima at 579 and 853 nm, respectively. UV/Vis spectra of the cluster in solution after ligand exchange with TPPMS and propanethiol show characteristics observed earlier in Au_8 and Au_{11} clusters respectively. As the electronic structure small gold nanoparticles evolve from the state of bulk continuum to discrete molecular orbital energy levels with decreasing size, such clusters may be attractive for application in nanodevices and molecular electronics.

Experimental Section

Au_9 Cluster Preparation: According to ref.[8a], $NaBH_4$ (0.018 g, 0.48 mmol) in ethanol (23 mL) was added dropwise into $Au(PPh_3)$-NO_3 (1.0 g, 1.9 mmol, prepared according to literature[18]) in ethanol (40 mL) whilst stirring. The mixture was stirred at room temperature for 2 h and then filtered. The dark red-brown filtrate was dried in vacuo and then dissolved in methylene dichloride (5 mL). After filtering and solvent evaporation under vacuum, the residue was washed with tetrahydrofuran and hexane. Finally drying in vacuo gave 0.27 g of green powder, $[Au_9(PPh_3)_8](NO_3)_3$ (**1**). The $^{31}P\{^1H\}$ spectrum of cluster **1** in CD_2Cl_2 gave one singlet at δ = 56.9 ppm. The crystal suitable for X-ray analysis, **1**·5CH_3OH, was obtained by a slow diffusion of diethyl ether into a cluster solution in methanol.

Structure Determination: Data were collected with Mo-K_α radiation (graphite monochromator, λ = 0.71073 Å) on a Bruker SMART D8 goniometer equipped with an APEX CCD detector; crystal size 0.34 × 0.23 × 0.15 mm, T = 153(2) K. Crystal data for **1**·5CH_3OH: $C_{149}H_{140}Au_9N_3O_{14}P_8$, formula mass 4217.10, orthorhombic space group *Ccce*, a = 25.786(2), b = 27.378(3), c = 19.2452(19) Å, V = 13587(2) Å^3, Z = 4, d_{calcd} = 2.062 mg m^{-3}, linear absorption coefficient 9.836 mm^{-1}, F(000) = 7992, 74317 reflections with $-30 \le h \le 31$, $-23 \le k \le 33$, $-14 \le l \le 23$, ω-scans, $2\theta_{max}$ = 51°, multiscan absorption correction[10b] (min. transmission 0.08, max. transmission 0.23), R_{int} = 0.1571. The structure was solved by direct methods.[10c] After assignment of the well-ordered electron-density maxima, a large void (103 Å^3) at Wyckoff position *4b* remained; the BYPASS procedure[10d] as implemented in PLATON[10a] indicated the presence of 59 electrons. Electron count and volume are in agreement with one nitrate anion and one molecule of solvent methanol per void; the overall composition matches the microanalytical data obtained for a crystalline sample. Refinement with full-matrix least-squares on F^2,[10e] anisotropic displacement parameters for Au and P, isotropic refinement for C, N, O, H atoms in structure factor calculations, convergence for 202 variables at wR_2 = 0.2376 (6336 reflections), R_1 = 0.1106 [6093 observations with $I > 2\sigma(I)$], gof = 1.268, residual electron density close to Au, +7.428/–4.387 e Å^{-3}.

Ligand Exchange Reaction Between 1 and Triphenylphosphane Monosulfonate Sodium Salt (TPPMS): A solution of TPPMS (7.5 mg, 1.9×10^{-2} mmol) in H_2O (3 mL) was added to a solution of cluster **1** (10 mg, 2.4×10^{-3} mmol) in CH_2Cl_2 (3 mL) and stirred at room temperature until the colour in the organic phase completely vanished. The red aqueous phase was ready for further use.

Ligand Exchange Reaction Between 1 and Propanethiol: A solution of propanethiol (13.5 mg, 1.7×10^{-1} mmol) in hexane (2 mL) was added to a solution of cluster **1** (8.0 mg, 1.9×10^{-3} mmol) in methanol (2 mL) and stirred at room temperature overnight. The colourless hexane layer was decanted and the dark brown methanol layer was dried in vacuo. After washing twice with ether and final drying, the solid was ready for further use.

Electrochemistry: Electrochemical analysis of **1** was performed with a Potentiostat Galvanostat Model 283 (Princeton Applied Research) using a platinum working electrode (diameter 1.0 cm), a platinum wire auxiliary electrode and a Hg/Hg_2Cl_2 (saturated KCl) reference electrode in an electrolyte solution of tetrabutylammonium hexafluorophosphate (TBHP) (0.1 M) in methylene dichloride. All measurements were conducted at room temperature.

UV/Vis Spectroscopy: UV/Vis spectra were collected with a J&M Tidas UV/Vis (Zeiss Axioplan 2) spectrometer. For the diffuse reflectance spectra of the microcrystals, cluster **1** was dissolved in methylene dichloride first and then dried on a glass slide in nitrogen.

Luminescence Spectroscopy: Photoluminescence spectra were taken on a luminescence spectrometer with a Nd:VO_4-laser source and an imaging Czerny–Turner monochromator. The sample was placed under a confocal microscope.

Transmission Electron Microscopy: Transmission electron microscopy (FEI Tecnai F20) was used to determine the particle size of cluster **1**. The sample was dissolved in ethanol and then transferred onto TEM grids coated with an ultrathin carbon layer.

CCDC-645243 (for **1**·5CH_3OH) contains supplementary crystallographic data. These data can be obtained free of charge from The Cambridge Crystallographic Data Centre via www.ccdc.cam.ac.uk/data_request/cif.

Acknowledgments

We thank our colleague Prof. Dr. U. Koelle for providing the equipment for the electrochemical measurements, and Dr. A. Sologubenko from the GFE at RWTH for TEM measurements. Furthermore, we are grateful to S. Luettjohann, M. Offer and Dr. H. Wiggers from the University Duisburg-Essen for the luminescence measurements. Financial support from the Deutsche Forschungsgemeinschaft (DFG) is gratefully acknowledged.

[1] a) S. W. Chen, R. S. Ingram, M. J. Hostetler, J. J. Pietron, R. W. Murray, T. G. Schaaff, J. T. Khoury, M. M. Alvarez, R. L. Whetten, *Science* **1998**, *280*, 2098–2101; b) G. Schmid, *Chem. Rev.* **1992**, *92*, 1709–1727; c) G. Schmid, U. Simon, *Chem. Commun.* **2005**, 697–710.

[2] a) H. Shiigi, Y. Yamamoto, N. Yoshi, H. Nakao, T. Nagaoka, *Chem. Commun.* **2006**, 4288–4290; b) H. M. Zareie, A. M.

McDonagh, J. Edgar, M. J. Ford, M. B. Cortie, M. R. Phillips, *Chem. Mater.* **2006**, *18*, 2376–2380; c) J. W. Zheng, P. E. Constantinou, C. Micheel, A. P. Alivisatos, R. A. Kiehl, N. C. Seeman, *Nano Lett.* **2006**, *6*, 1502–1504; d) O. Lioubashevski, V. I. Chegel, F. Patolsky, E. Katz, I. Willner, *J. Am. Chem. Soc.* **2004**, *126*, 7133–7143; e) B. R. Walker, R. A. Wassel, D. M. Stefanescu, C. B. Gorman, *J. Am. Chem. Soc.* **2004**, *126*, 16330–16331; f) D. Kruger, R. Rousseau, H. Fuchs, D. Marx, *Angew. Chem. Int. Ed.* **2003**, *42*, 2251–2253; g) U. Simon, *Adv. Mater.* **1998**, *10*, 1487–1492.

[3] a) J. P. Wilcoxon, J. E. Martin, F. Parsapour, B. Wiedenman, D. F. Kelley, *J. Chem. Phys.* **1998**, *108*, 9137–9143; b) S. Link, A. Beeby, S. FitzGerald, M. A. El-Sayed, T. G. Schaaff, R. L. Whetten, *J. Phys. Chem. B* **2002**, *106*, 3410–3415; c) Y. Negishi, T. Tsukuda, *Chem. Phys. Lett.* **2004**, *383*, 161–165; d) J. Zheng, J. T. Petty, R. M. Dickson, *J. Am. Chem. Soc.* **2003**, *125*, 7780–7781.

[4] J. J. Steggerda, J. J. Bour, J. W. A. van der Velden, *Recl. Trav. Chim. Pays-Bas* **1982**, *101*, 164–170.

[5] M. Schulz-Dobrick, M. Jansen, *Eur. J. Inorg. Chem.* **2006**, 4498–4502.

[6] F. Wen, U. Englert, M. Homberger, U. Simon, *Z. Anorg. Allg. Chem.* **2006**, 2159.

[7] K. P. Hall, D. M. P. Mingos, *Prog. Inorg. Chem.* **1984**, *32*, 237–325.

[8] a) P. L. Bellon, F. Cariati, M. Manassero, L. Naldini, M. Sansoni, *J. Chem. Soc. Chem. Commun.* **1971**, 1423–1424; b) K. P. Hall, B. R. C. Theobald, D. I. Gilmour, D. Michael, P. Mingos, A. J. Welch, *J. Chem. Soc. Chem. Commun.* **1982**, 528–530; c) C. E. Briant, K. P. Hall, D. M. P. Mingos, *J. Chem. Soc. Chem. Commun.* **1984**, 290–291.

[9] J. W. A. Vandervelden, J. J. Bour, W. P. Bosman, J. H. Noordik, *Inorg. Chem.* **1983**, *22*, 1913–1918.

[10] a) A. L. Spek, *J. Appl. Crystallogr.* **2003**, *36*, 7–13; b) G. M. Sheldrick, *SADABS*, Program for Empirical Absorption Correction of Area Detector Data., University of Göttingen, Göttingen, **1996**; c) G. M. Sheldrick, *SHELXS97*, Program for Crystal Structure Solution, University of Göttingen, Göttingen, **1997**; d) P. van der Sluis, A. L. Spek, *Acta Crystallogr., Sect. A* **1990**, *46*, 194–201; e) G. M. Sheldrick, *SHELXL97*, Program for Crystal Structure Refinement, University of Göttingen, Göttingen, **1997**; f) T. G. Schaaff, M. N. Shafigullin, J. T. Khoury, I. Vezmar, R. L. Whetten, W. G. Cullen, P. N. First, C. Gutierrez-Wing, J. Ascensio, M. J. Jose-Yacaman, *J. Phys. Chem. B* **1997**, *101*, 7885–7891.

[11] a) H. R. C. Jaw, W. R. Mason, *Inorg. Chem.* **1991**, *30*, 275–278; b) D. M. P. Mingos, *Polyhedron* **1984**, *3*, 1289–1297.

[12] F. A. Vollenbroek, W. P. Bosman, J. J. Bour, J. H. Noordik, P. T. Beurskens, *J. Chem. Soc. Chem. Commun.* **1979**, 387–388.

[13] a) L. O. Brown, J. E. Hutchison, *J. Am. Chem. Soc.* **1997**, *119*, 12384–12385; b) M. G. Warner, S. M. Reed, J. E. Hutchison, *Chem. Mater.* **2000**, *12*, 3316–3320.

[14] a) G. H. Woehrle, J. E. Hutchison, *Inorg. Chem.* **2005**, *44*, 6149–6158; b) Y. Y. Yang, S. W. Chen, *Nano Lett.* **2003**, *3*, 75–79; Y. Shichibu, Y. Negishi, T. Watanabe, N. K. Chaki, H. Kawaguchi, T. Tsukuda, *J. Phys. Chem. C* **2007**, *111*, 7845–7847.

[15] a) J. H. Chen, A. A. Mohamed, H. E. Abdou, J. A. K. Bauer, J. P. Fackler, A. E. Bruce, M. R. M. Bruce, *Chem. Commun.* **2005**, 1575–1577; b) B. I. Ipe, K. Yoosaf, K. G. Thomas, *J. Am. Chem. Soc.* **2006**, *128*, 1907–1913; c) V. L. Jimenez, D. G. Georganopoulou, R. J. White, A. S. Harper, A. J. Mills, D. I. Lee, R. W. Murray, *Langmuir* **2004**, *20*, 6864–6870; d) Y. Negishi, Y. Takasugi, S. Sato, H. Yao, K. Kimura, T. Tsukuda, *J. Am. Chem. Soc.* **2004**, *126*, 6518–6519; e) V. W. W. Yam, E. C. C. Cheng, K. K. Cheung, *Angew. Chem. Int. Ed.* **1999**, *38*, 197–199; f) V. W. W. Yam, E. C. C. Cheng, Z. Y. Zhou, *Angew. Chem. Int. Ed.* **2000**, *39*, 1683–1685; g) C.-C. Huang, Z. Yang, K.-H. Lee, H. T. Chang, *Angew. Chem.* **2007**, *119*, 6948–6952.

[16] G. M. J. van der Linden, L. H. M. Paulissen, J. E. J. Schmitz, *J. Am. Chem. Soc.* **1983**, *105*, 1903–1907.

[17] a) L. D. Menard, S. P. Gao, H. P. Xu, R. D. Twesten, A. S. Harper, Y. Song, G. L. Wang, A. D. Douglas, J. C. Yang, A. I. Frenkel, R. G. Nuzzo, R. W. Murray, *J. Phys. Chem. B* **2006**, *110*, 12874–12883; b) R. Balasubramanian, R. Guo, A. J. Mills, R. W. Murray, *J. Am. Chem. Soc.* **2005**, *127*, 8126–8132; c) B. M. Quinn, P. Liljeroth, V. Ruiz, T. Laaksonen, K. Kontturi, *J. Am. Chem. Soc.* **2003**, *125*, 6644–6645.

[18] A. M. Mueting, B. D. Alexander, P. D. Boyle, A. L. Casalnuovo, L. N. Ito, B. J. Johnson, L. H. Pignolet, *Inorg. Synth.* **1992**, *29*, 279–298.

Received: May 22, 2007
Published Online: November 30, 2007

